The N-peptide–binding mode is critical to Munc18-1 function in synaptic exocytosis

Received for publication, August 7, 2018, and in revised form, September 25, 2018 Published, Papers in Press, October 1, 2018, DOI 10.1074/jbc.RA118.005254

Chong Shen[‡1], Yinghui Liu[‡§1], Haijia Yu[‡§2], Daniel R. Gulbranson[‡], Igor Kogut[¶], Ganna Bilousova[¶], Chen Zhang[‖], Michael H. B. Stowell[‡], and Jingshi Shen[‡3]

From the [‡]Department of Molecular, Cellular, and Developmental Biology, University of Colorado, Boulder, Colorado 80309, the [§]Jiangsu Key Laboratory for Molecular and Medical Biotechnology, College of Life Sciences, Nanjing Normal University, Nanjing 210023, China, the [¶]Department of Dermatology and Charles C. Gates Center for Regenerative Medicine, University of Colorado School of Medicine, Aurora, Colorado 80045, and the [‖]School of Basic Medical Sciences, Capital Medical University, Beijing 100069, China

Edited by Phyllis I. Hanson

Sec1/Munc18 (SM) proteins promote intracellular vesicle fusion by binding to *N*-ethylmaleimide–sensitive factor attachment protein receptors (SNAREs). A key SNARE-binding mode of SM proteins involves the N-terminal peptide (N-peptide) motif of syntaxin, a SNARE subunit localized to the target membrane. In *in vitro* membrane fusion assays, inhibition of N-peptide motif binding previously has been shown to abrogate the stimulatory function of Munc18-1, a SM protein involved in synaptic exocytosis in neurons. The physiological role of the N-peptide–binding mode, however, remains unclear. In this work, we addressed this key question using a "clogged" Munc18-1 protein, in which an ectopic copy of the syntaxin N-peptide motif was directly fused to Munc18-1. We found that the ectopic N-peptide motif blocks the N-peptide–binding pocket of Munc18-1, preventing the latter from binding to the native N-peptide motif on syntaxin-1. In a reconstituted system, we observed that clogged Munc18-1 is defective in promoting SNARE zippering. When introduced into induced neuronal cells (iN cells) derived from human pluripotent stem cells, clogged Munc18-1 failed to mediate synaptic exocytosis. As a result, both spontaneous and evoked synaptic transmission was abolished. These genetic findings provide direct evidence for the crucial role of the N-peptide–binding mode of Munc18-1 in synaptic exocytosis. We suggest that clogged SM proteins will also be instrumental in defining the physiological roles of the N-peptide–binding mode in other vesicle-fusion pathways.

This work was supported by National Basic Research Program of China Grant 2017YFA0105201 and National Science Foundation of China Grant 31670842 (both to C. Z.), National Science Foundation of China Grant 31871425 (to H. Y.), National Institutes of Health Grants GM126960 and DK095367 (both to J. S.), a University of Colorado seed grant (to J. S.), and an American Heart Association predoctoral fellowship (to D. R. G.). The authors declare that they have no conflicts of interest with the contents of this article. The content is solely the responsibility of the authors and does not necessarily represent the official views of the National Institutes of Health.

This article contains Table S1 and Figs. S1–S4.

[1] Both authors contributed equally to this work.
[2] To whom correspondence may be addressed. E-mail: haijiayu@gmail.com.
[3] To whom correspondence may be addressed. E-mail: jingshi.shen@colorado.edu.

Intracellular vesicle fusion in eukaryotes requires two conserved classes of molecules: SNAREs[4] and SM proteins (1–3). The vesicle-fusion reaction is initiated when the vesicle-anchored v-SNARE pairs with its cognate target membrane-associated t-SNAREs to form a trans-SNARE complex (SNAREpin) (4–7). The trans-SNARE complex zippers progressively toward the lipid bilayers, forcing the membranes into close proximity to fuse (8–12). SM proteins are soluble factors of 60–70 kDa that control vesicle fusion by binding to their cognate SNAREs (13–18). One of the best-studied vesicle-fusion pathway is synaptic exocytosis, which mediates the release of neurotransmitters at chemical synapses in the nervous system (19–21). Synaptic exocytosis requires syntaxin-1 and SNAP-25 as the t-SNAREs, VAMP2/synaptobrevin-2 as the v-SNARE, and Munc18-1/STXBP1/nSec1 as the cognate SM protein (4, 22–28).

A conserved function of SM proteins is to regulate the zippering of the trans-SNARE complex in the vesicle-fusion reaction (14, 18, 29–34). While supplying the energy for membrane merging, SNAREs alone zipper inefficiently (18, 35). By recognizing sequences on both the v- and t-SNAREs, SM proteins promote the zippering of the trans-SNARE complex and accelerate the kinetics of SNARE-dependent fusion reactions (18, 36–39). SM proteins selectively activate their cognate SNARE pairs, thus augmenting the compartmental specificity of intracellular vesicle fusion (18, 35, 40).

A key SNARE-SM binding mode involves the N-terminal peptide (N-peptide) motif located at the extreme N terminus of syntaxin (14, 18, 36, 37, 41, 42). Characterized by multiple charged residues and a hydrophobic leucine or phenylalanine residue (Fig. 1*A*), the N-peptide motif is accommodated within a peripheral pocket on the SM protein (43–45). The N-peptide motif recruits the soluble SM protein to the vicinity of membrane-anchored SNAREs, facilitating the interaction between the SM protein and the trans-SNARE complex (37). In reconstituted fusion assays, the N-peptide–binding mode is critical

[4] The abbreviations used are: SNARE, *N*-ethylmaleimide–sensitive factor attachment protein receptor; SM, Sec1/Munc18; N-peptide, N-terminal peptide; iN cells, induced neuronal cells; iPSC, induced pluripotent stem cell; shRNA, short hairpin RNA; KO, knockout; gRNA, guide RNA; EPSC, excitatory postsynaptic current; mEPSC, miniature excitatory postsynaptic current; NTD, N-terminal domain; DIC, differential interference contrast.

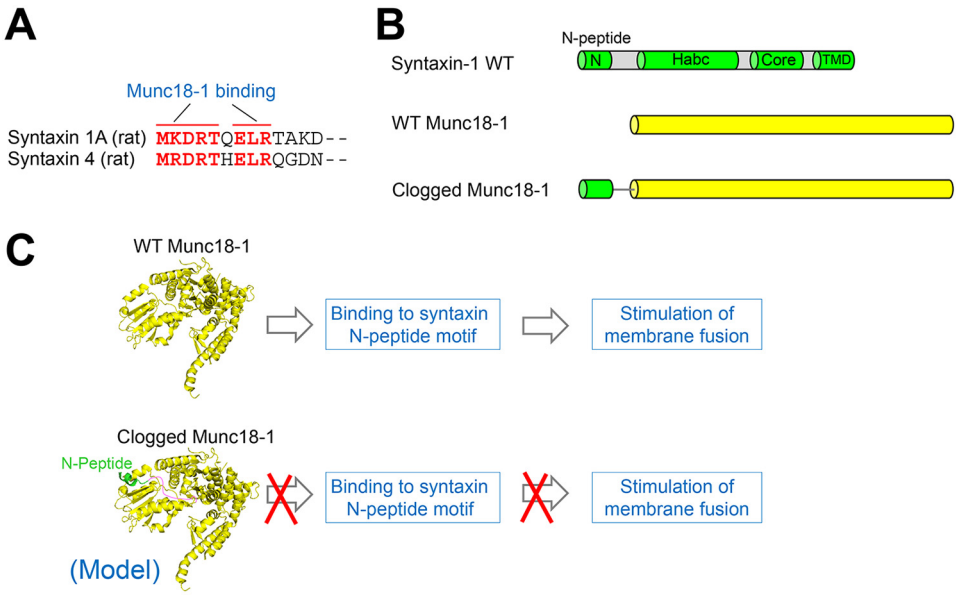

Figure 1. Illustration of the clogged Munc18-1 strategy. *A*, sequence alignment of syntaxin-1A and syntaxin-4 with conserved residues in the N-peptide motifs highlighted. Hereafter, syntaxin-1A is referred to as syntaxin-1. *B*, syntaxin-1 and Munc18-1 (WT or clogged). The domains of syntaxin-1 are shown. *N*, N-peptide motif; *Habc*, N-terminal Habc regulatory domain; *Core*: SNARE core domain (SNARE motif); *TMD*, transmembrane domain. *C*, model depicting the activities of WT and clogged Munc18-1 proteins in SNARE-dependent membrane fusion based on reconstitution studies (37). *Yellow*, Munc18-1; *green*, the N-terminal sequence of syntaxin-1 (amino acids 1–30) containing the N-peptide motif; *purple*, an engineered linker (23 residues). The model is based on the crystal structure of Munc18-1 complexed with the N-peptide motif of syntaxin-4 (Protein Data Bank code 3PUJ). Key residues of the N-peptide motif are conserved in syntaxin-1 and syntaxin-4. The sequence of the clogged Munc18-1 protein is included under "Experimental procedures."

to the stimulatory function of Munc18-1 (18, 36, 37). The physiological function of this N-peptide–binding mode in neurons, however, has been debated. In genetic studies using cultured neurons or whole animals, mutations in either the syntaxin N-peptide or the N-peptide–binding pocket of Munc18-1 strongly inhibited synaptic exocytosis (46–48). In other genetic studies, however, such mutations had little impact on synaptic exocytosis (49–51). The discrepancy of these genetic data are likely due to the intrinsic limitations of point mutations, which often do not completely inhibit the N-peptide–binding mode and/or may cause protein misfolding. Thus, a new approach is needed to examine the physiological function of the N-peptide–binding mode of Munc18-1 in synaptic exocytosis.

In this work, we took advantage of a "clogged" Munc18-1 protein in which an ectopic copy of the syntaxin N-peptide motif is directly fused to Munc18-1 to block its N-peptide–binding pocket (37). The clogged Munc18-1 protein is unable to bind the native N-peptide motif on syntaxin and thus fails to stimulate SNARE-dependent membrane fusion *in vitro* (37). Using a reconstituted system, we found that clogged Munc18-1 failed to promote trans-SNARE zippering. When introduced into induced neuronal (iN) cells differentiated from human induced pluripotent stem cells (iPSCs), clogged Munc18-1 was defective in mediating synaptic exocytosis. Thus, both spontaneous and evoked synaptic transmission were abrogated. Consistent with our reconstitution data, these genetic results demonstrated that the N-peptide–binding mode is indispensable to Munc18-1 function in synaptic exocytosis.

Results

In our previous biochemical studies, we engineered a clogged Munc18-1 protein in which an ectopic copy of the N-peptide motif from syntaxin-1 was directly fused to the N terminus of Munc18-1 through a flexible linker (Fig. 1, *B* and *C*) (37). The ectopic N-peptide motif occupies the N-peptide–binding pocket of Munc18-1 and prevents the latter from binding to the native N-peptide motif on syntaxin-1. As a result, the clogged Munc18-1 protein is unable to stimulate SNARE-dependent membrane fusion *in vitro* (Fig. 1, *B* and *C*) (37). To gain further mechanistic insights into the clogged Munc18-1 protein, we first examined its regulatory activity in trans-SNARE zippering *in vitro*. Synaptic exocytic SNAREs alone zippered poorly in a trans-SNARE assembly assay (Fig. 2 (*A* and *B*) and Fig. S1). The addition of WT Munc18-1 strongly accelerated the zippering kinetics (Fig. 2 (*A* and *B*) and Fig. S1). The clogged Munc18-1 protein, by contrast, was completely inactive in regulating the zippering process, resulting in near-background levels of trans-SNARE zippering (Fig. 2 (*A* and *B*) and Fig. S1). Next, we examined how clogged Munc18-1 regulates the upstream docking step of SNAREs. We observed that, like WT Munc18-1, clogged Munc18-1 did not influence the initial docking of SNAREs (Fig. 2, *C* and *D*). The CD spectra of WT and clogged Munc18-1 proteins were very similar (Fig. 2*E*), suggesting that clogged Munc18-1 was properly folded. These results demonstrated that clogged Munc18-1 is defective in promoting trans-SNARE zippering, providing a molecular explanation for its inability to accelerate the kinetics of SNARE-dependent membrane fusion.

The clogged Munc18-1 protein offered an ideal opportunity to examine the physiological role of the N-peptide–binding mode in synaptic exocytosis. First of all, the ectopic N-peptide motif completely blocks the N-peptide–binding pocket of Munc18-1 *in vitro* (Fig. 2, *A* and *B*) (37), in contrast to point mutations that may incompletely inhibit N-peptide binding to

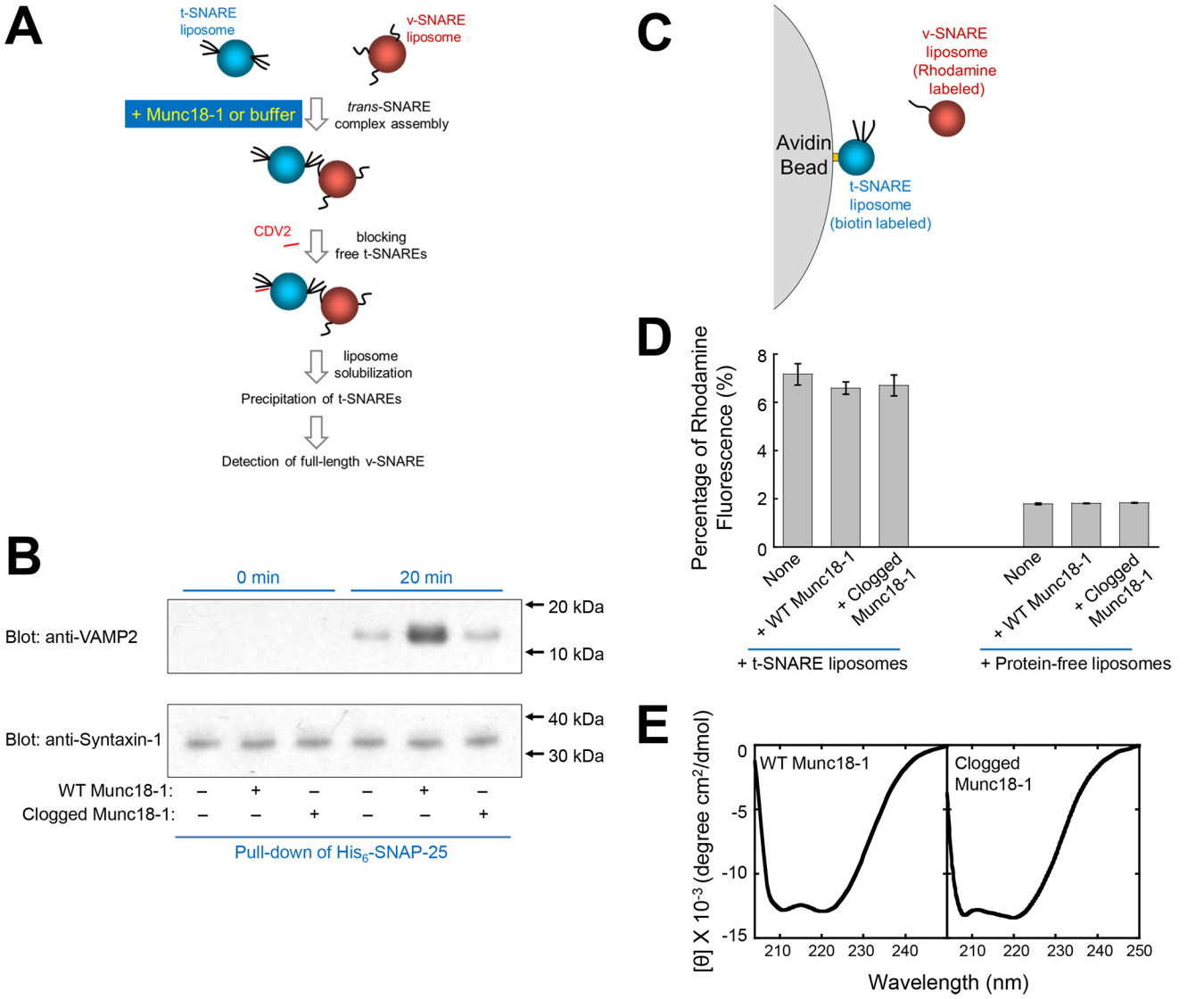

Figure 2. Clogged Munc18-1 is defective in promoting trans-SNARE zippering. *A*, the trans-SNARE assembly assay (52). Reconstituted t- and v-SNARE liposomes were incubated at 4 °C for the indicated durations before a 10-fold excess amount of inhibitory CDV2 was added to block unpaired t-SNAREs. The liposomes were subsequently solubilized, and the t-SNAREs were precipitated using nickel-Sepharose beads. Levels of full-length VAMP2 in the precipitates were measured by immunoblotting and used as an indicator for trans-SNARE assembly between liposomes. The reactions were performed in the presence of 100 mg/ml Ficoll 70. *B*, immunoblots showing syntaxin-1 and VAMP2 protein levels in the precipitates from the trans-SNARE assembly assays. Additional analyses of the trans-SNARE complexes are included in Fig. S1. *C*, the liposome docking assay was performed as described previously (35). The biotin-labeled t-SNARE liposomes containing syntaxin-1 and SNAP-25 were anchored to avidin beads and used to pull down rhodamine-labeled v-SNARE liposomes. A VAMP2NTD-TolA chimera was used as the v-SNARE in the docking assay to selectively assess the NTD-mediated docking step (66). The binding reactions were performed at 4 °C for 1 h in the absence or presence of 5 μM Munc18-1 (WT or clogged). *D*, effects of WT and clogged Munc18-1 proteins on liposome docking. Data are presented as percentage of rhodamine fluorescence intensity. Binding reactions containing biotin-labeled, protein-free liposomes were included to show the background fluorescence signals (SNARE-independent liposome docking). *Error bars*, S.D. *E*, CD spectroscopic analysis of WT and clogged Munc18-1 proteins. The CD spectra were measured using a Jasco J-815 spectropolarimeter equipped with a 1-mm quartz cell. The readings were made at 0.5-nm intervals, and each *data point* represents the average of six scans at a speed of 50 nm/min over the wavelength range of 200–250 nm. The data were converted into mean residue weighted molar ellipticity using the equation, $[\theta] = (100 \times \theta)/CnI$, where C is the protein concentration (mM), θ is the measured ellipticity (millidegrees), n is the number of residues, and l is the path length (cm).

Munc18-1. Moreover, clogged Munc18-1 does not harbor any mutation in the Munc18-1 sequence. This is important because the folding of Munc18-1 protein is highly sensitive to perturbations, including single-residue substitutions (18). Thus, mutations in the N-peptide–binding pocket of Munc18-1 may cause local misfolding of the protein, complicating functional analyses.

To determine the activity of clogged Munc18-1 in neurons, endogenous Munc18-1 needs to be eliminated and replaced with clogged Munc18-1. Our initial plan was to silence Munc18-1 expression in primary mouse cortical neurons using short hairpin RNA (shRNA), similar to a strategy used in our genetic dissection of the synaptic v-SNARE VAMP2 (52). However, we found that this shRNA method did not fully abrogate Munc18-1 expression in neurons. In this work, we characterized the clogged Munc18-1 protein in iN cells derived from human iPSCs (Fig. 3*A*) (53). Lentiviral expression of the transcription factor Ngn2 rapidly and efficiently (nearly 100%) programmed human iPSCs into iN cells (Fig. 3, *B–D*) (53). As demonstrated in this work and previous studies (53, 54), iN cells

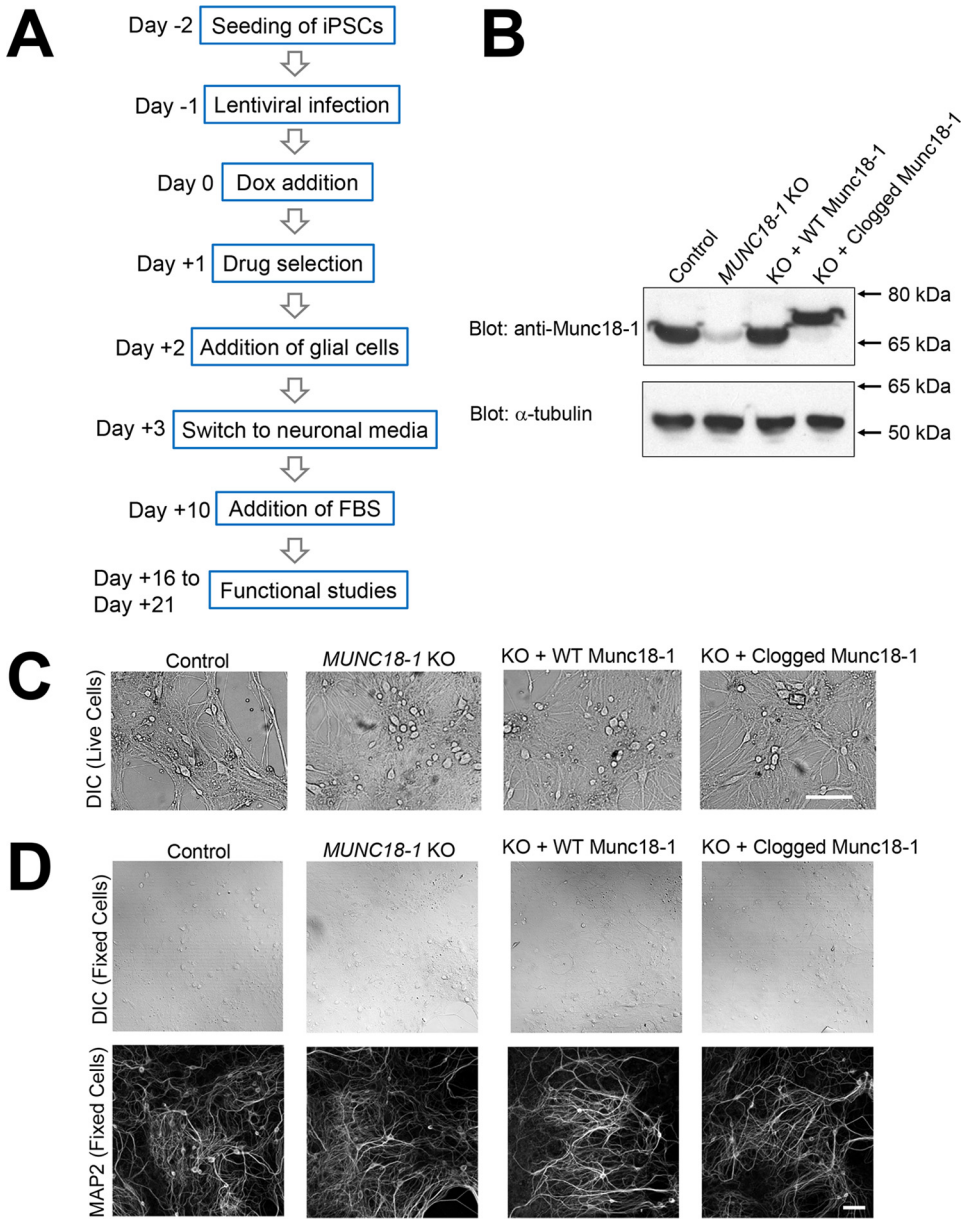

Figure 3. Expression of clogged Munc18-1 in human iN cells derived from iPSCs. *A*, flowchart depicting the procedure of programming human iPSCs into iN cells (53). *B*, immunoblots showing the expression of MUNC18-1 in iN cells. The *MUNC18-1* gene was deleted in iPSCs using CRISPR/Cas9. In rescue experiments, the *MUNC18-1* KO iPSCs were infected with lentiviruses expressing WT or mutant Munc18-1 proteins. The iPSCs were then differentiated into iN cells. *Control*, iN cells derived from WT iPSCs. The expression of α-tubulin was used as a loading control. *C*, DIC images showing live iN cells at day 16. The images were acquired on a Carl Zeiss AxioObserver Z1 microscope. *Scale bar*, 100 μm. *D*, DIC (*top*) and fluorescent (*bottom*) images showing fixed iN cells at day 18. In the fluorescent images, the neuronal marker MAP2 is labeled. The images were acquired on a Carl Zeiss LSM 510 confocal microscope. *Scale bar*, 100 μm. The numbers of viable iN cells were similar across the populations at the time of functional analyses. *FBS*, fetal bovine serum.

were morphologically and functionally similar to primary excitatory cortical neurons. Because gene KO and rescue were carried out in iPSCs, we could generate virtually unlimited supplies of iN cells with defined genetic alterations. We used CRISPR/Cas9 genome editing to ablate the *MUNC18-1* gene in the iPSCs. Rescue genes expressing WT or clogged Munc18-1 were expressed in *MUNC18-1* KO iPSCs using lentiviral expression. The iPSCs were then differentiated into iN cells (Fig. 3*A*).

To rule out clonal variations of iPSCs, we chose to generate iN cells using pooled KO iPSCs. CRISPR genome editing is expected to be particularly effective for *MUNC18-1* KO because the stability of Munc18-1 protein is highly sensitive to perturbations (18). Thus, even in-frame indel mutations will likely create loss-of-function alleles. Indeed, MUNC18-1 expression in iN cells was abolished by CRISPR genome editing using a guide RNA (gRNA) targeting an early exon of the *MUNC18-1* gene (Fig. 3*B*).

The suitability of this iN cell system for genetic dissection of Munc18-1 function is supported by four lines of evidence. First, similar amounts of iN cells were used for functional analysis across the experiments. Because *MUNC18-1* KO reduces the viability of neurons (28, 55), the numbers of seeded iPSCs were adjusted to achieve similar densities of iN cell populations at the time of functional measurements (Fig. 3, *C* and *D*). The

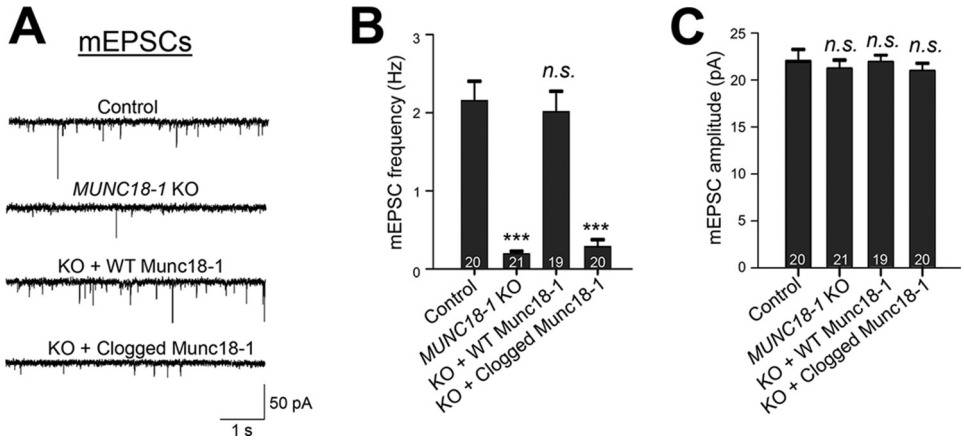

Figure 4. Clogged Munc18-1 is unable to mediate spontaneous synaptic releases. *A*, representative traces of mEPSCs, which reflected spontaneous synaptic vesicle fusion. *B*, summary graph of mEPSC frequency. Numbers of recorded cells are listed on the *bars*. Numbers of neurons and independent cultures are listed in Table S1. Statistical analysis was performed using Student's *t* test comparing a test data set with the control experiment of WT cells. Data shown in summary graphs are mean ± S.E. (*error bars*). ***, $p < 0.001$. *n.s.*, not significant. *C*, summary graph of mEPSC amplitudes. Data shown in summary graphs are mean ± S.E. *n.s.*, not significant. Scatter plots of *B* and *C* are show in Fig. S4*A*.

expression levels of α-tubulin were comparable across the iN cell populations (Fig. 3*B*), confirming our cell density estimation. Second, the overall morphologies of the WT and mutant iN cells were similar without apparent cell death (Fig. 3, *C* and *D*). Third, the expression levels of the rescue Munc18-1 (WT or clogged) were comparable with endogenous Munc18-1 expression (Fig. 3*B*). Finally, the phenotype of the *MUNC18-1* KO iN cells was similar to that of primary neurons isolated from *Munc18-1* KO mice, and the phenotype could be fully rescued by the WT *Munc18-1* gene (see below).

We then examined synaptic neurotransmitter releases in the iN cells using electrophysiological measurements. We first measured miniature excitatory postsynaptic currents (mEPSCs), which reflected spontaneous neurotransmitter releases. As expected, KO of *MUNC18-1* strongly reduced the frequency of mEPSCs in iN cells (Fig. 4, *A* and *B*). The frequency of mEPSCs was fully rescued by the WT *Munc18-1* gene but not by the gene encoding clogged Munc18-1 (Fig. 4, *A* and *B*). The amplitudes of mEPSCs were similar in all the iN cell populations (Fig. 4*C*), suggesting that the loading of neurotransmitters into synaptic vesicles was unchanged. These results demonstrated that clogged Munc18-1 failed to mediate spontaneous synaptic releases.

Next, we measured evoked excitatory postsynaptic currents (EPSCs) in the iN cells, which reflected evoked neurotransmitter releases. *MUNC18-1* KO strongly decreased the amplitudes of EPSCs triggered by local electrical stimulation (Fig. 5). The EPSCs were fully restored by the expression of WT Munc18-1 but not by clogged Munc18-1 (Fig. 5). Thus, the clogged Munc18-1 protein was unable to mediate evoked synaptic neurotransmitter release.

To rule out potential off-target effects of CRISPR genome editing, we designed another two gRNAs targeting early exons of the *MUNC18-1* gene. These two gRNAs were simultaneously introduced into iPSCs to mutate the *MUNC18-1* gene. WT and clogged Munc18-1 were then expressed in the KO iPSCs before the cells were differentiated into iN cells. Immunoblotting of the iN cells showed that MUNC18-1 expression was eliminated in the KO cells, whereas WT and clogged Munc18-1 proteins were expressed to the endogenous level of MUNC18-1 (Fig. S2*A*). Electrophysiological measurements showed that the frequency of mEPSCs was severely diminished in the KO iN cells (Fig. S2, *B* and *C*). The frequency of mEPSCs was fully rescued by the expression of WT Munc18-1 but not by clogged Munc18-1 (Fig. S2, *B* and *C*). Likewise, the amplitudes of evoked EPSCs were strongly reduced in the *MUNC18-1* KO iN cells (Fig. S3). The EPSCs were fully restored by WT Munc18-1 but not by clogged Munc18-1 (Fig. S3). These findings are consistent with the results of the genetic experiments using a single gRNA (Figs. 4 and 5), indicating that the phenotype of the mutant cells was due to specific loss-of-function mutations in the *MUNC18-1* gene.

Together, these genetic data demonstrated that clogged Munc18-1 is defective in mediating synaptic exocytosis in neurons, correlating with its inability to promote trans-SNARE zippering *in vitro*. Thus, we conclude that the N-peptide–binding mode is crucial to Munc18-1 function in synaptic exocytosis.

Discussion

A major discovery of our previous reconstitution studies was that the SM protein Munc18-1 promotes SNARE-dependent membrane fusion, and its stimulatory function requires binding to the N-peptide motif of syntaxin-1 (18, 36, 37). In this study, we provided direct genetic evidence for the crucial role of the N-peptide–binding mode in synaptic exocytosis in neurons. Our findings also further support the notion that the N-peptide motif promotes membrane fusion by facilitating the association between Munc18-1 and the membrane-anchored SNARE complex, rather than allosterically activating Munc18-1.

Our genetic data helped resolve a major controversy in the field regarding the physiological role of the N-peptide–binding mode. The binding of the N-peptide motif to Munc18-1 involves a number of intermolecular interactions (44). In other genetic studies, point mutations were introduced to disrupt a subset of these interactions, which was expected to reduce but not abolish the N-peptide binding. Partial inhibition of N-peptide binding may lead to variable consequences *in vivo*, strongly dependent on experimental conditions such as protein expression levels. Extensive mutations of the N-peptide–Munc18-1

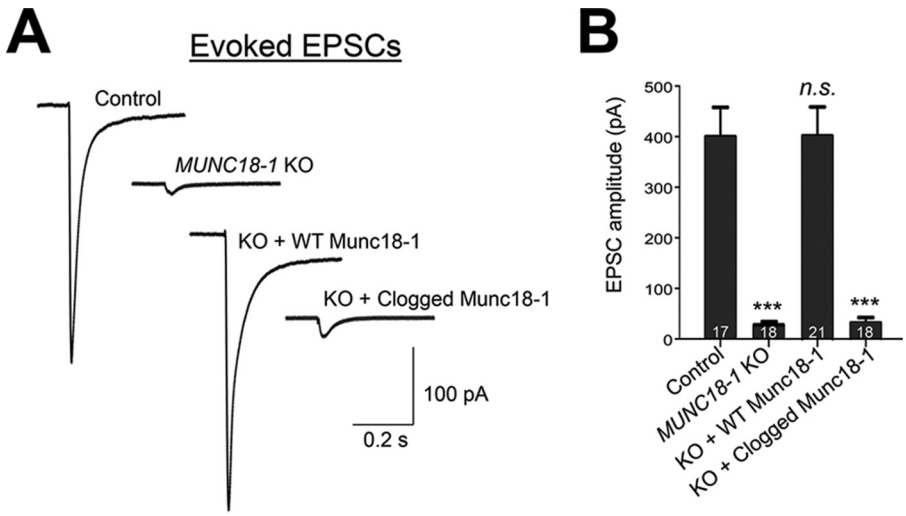

Figure 5. Clogged Munc18-1 fails to mediate evoked synaptic releases. *A*, representative traces of EPSCs evoked by local electrical stimulation in iN cells. *B*, summary graph of EPSC amplitudes. Data shown in the summary graphs are mean ± S.E. (*error bars*). ***, $p < 0.001$. *n.s.*, not significant. Numbers of recorded cells are listed on the *bars*. Numbers of neurons and independent cultures are listed in Table S1. Statistical analysis was performed using Student's *t* test comparing a test data set with the control experiment of WT cells. A scatter plot of *C* is shown in Fig. S4*B*.

interactions, on the other hand, likely cause local misfolding of the protein, and the folding state may differ across experimental systems, contributing to conflicting phenotypes.

Although we cannot completely exclude the possibility that the N-peptide–binding pocket of Munc18-1 also recognizes another molecule, we consider this scenario unlikely. The N-peptide motif of syntaxin is a highly specialized sequence not known to exist in other vesicle-fusion regulators. Moreover, the peripheral N-peptide–binding pocket of Munc18-1 is physically separate from other SNARE-binding regions (*e.g.* domain 3a) and is not known to associate with other molecules. Nevertheless, SNAREs and Munc18-1 are known to bind other regulatory factors, including Munc13 (31, 56). Further research will be needed to determine whether and how the N-peptide–binding mode is influenced by Munc13 and other regulatory factors. Likewise, additional studies will be required to examine whether the ectopic N-peptide motif binds Munc18-1 in a similar way as the native N-peptide.

Whereas the N-peptide–binding mode is widespread in vesicle fusion, it is absent in certain SM proteins, including the yeast exocytic SM protein Sec1p. For these SM proteins, the recruitment role of the N-peptide motif is likely fulfilled by another SNARE–SM binding mode or by a regulatory protein physically linking the SM protein and SNAREs.

We suggest that clogged SM protein is a powerful approach to determine the functional roles of the N-peptide–binding mode in other vesicle-fusion pathways both *in vitro* and *in vivo*. For example, the N-peptide motif of syntaxin-4 is recognized by Munc18c/Munc18-3, a SM protein involved in insulin-stimulated GLUT4 exocytosis in adipocytes and skeletal muscles (35, 57–59). It is still unclear whether N-peptide binding is required for Munc18c function in GLUT4 exocytosis. Like neurons, adipocytes and skeletal muscles are post-mitotic cells difficult to genetically manipulate in culture. Recently, human iPSCs have been successfully programmed into functional adipocytes and muscle cells (60–62). Thus, the gene KO and rescue strategy described in this study will be instrumental in characterizing the regulatory activities of clogged Munc18c in iPSC-derived adipocytes and muscle cells.

Experimental procedures

Recombinant protein expression and purification

Recombinant proteins were expressed and purified from *Escherichia coli* using nickel-affinity chromatography (37, 52). The synaptic exocytic t-SNARE complex was composed of untagged rat syntaxin-1 and mouse SNAP-25 with an N-terminal His_6 tag (36). The sequence of the clogged Munc18-1 protein used in this work is as follows (the syntaxin-1 sequence containing the N-peptide motif is underlined, whereas the linker sequence is shown in boldface type): MKDRTQELRTAKDSDDDDVTVTVDRDRFM**GGGGGGGGGGSRYPYDVPDYAKL**MAPIGLKAVVGEKIMHDVIKKVKKKGEWKVLVVDQLSMRMLSSCCKMTDIMTEGITIVEDINKRREPLPSLEAVYLITPSEKSVHSLISDFKDPPTAKYRAAHVFFTDSCPDALFNELVKSRAAKVIKTLTEINIAFLPYESQVYSLDSADSFQSFYSPHKAQMKNPILERLAEQIATLCATLKEYPAVRYRGEYKDNALLAQLIQDKLDAYKADDPTMGEGPDKARSQLLILDRGFDPSSPVLHELTFQAMSYDLLPIENDVYKYETSGIGEARVKEVLLDEDDDLWIALRHKHIAEVSQEVTRSLKDFSSSKRMNTGEKTTMRDLSQMLKKMPQYQKELSKYSTHLHLAEDCMKHYQGTVDKLCRVEQDLAMGTDAEGEKIKDPMRAIVPILLDANVSTYDKIRIILLYIFLKNGITEENLNKLIQHAQIPPEDSEIITNMAHLGVPIVTDSTLRRRSKPERKERISEQTYQLSRWTPIIKDIMEDTIEDKLDTKHYPYISTRSSASFSTTAVSARYGHWHKNKAPGEYRSGPRLIIFILGGVSLNEMRCAYEVTQANGKWEVLIGSTHILTPQKLLDTLKKLNKTDEEISS.

The sequence of the VAMP2NTD-TolA chimera, in which the C-terminal domain of VAMP2 was replaced with a bacterial TolA sequence, is as follows (TolA sequence is underlined): MSATAATVPPAAPAGEGGPPAPPPNLTSNRRLQQTQAQVDEVVDIMRVNVDKVLERDQKGGSSIDAVMVDSGAVVEQYKRMQSQKRKYWWKNLKMMIILGVICAIILIIIVYFST.

Trans-SNARE assembly assay

The v- and t-SNARE liposomes were prepared as described previously (35, 63, 64). The v- and t-SNARE liposomes were incubated at 4 °C for the indicated durations in the presence or absence of 5 μM Munc18-1 before a 10-fold excess amount of inhibitory VAMP2 cytosolic domain (CDV2) was added. Each reaction contained 5 μM t-SNAREs and 1.5 μM t-SNARE. The liposomes were solubilized with 1% CHAPS, and the t-SNAREs were precipitated using nickel-Sepharose beads through binding to the His_6 tag on SNAP-25. The levels of full-length VAMP2 proteins in the precipitates were measured by immunoblotting using monoclonal anti-VAMP2 antibodies (clone Cl69.1, Synaptic Systems), which was used as an indicator for trans-SNARE assembly between liposomes. Syntaxin-1 was detected using monoclonal anti-syntaxin-1 antibodies (clone HPC-1, Synaptic Systems).

Liposome docking assay

SNARE liposomes were prepared in a similar way as in the trans-SNARE assembly assay except that 2% biotin-conjugated 1-(12-biotinyl(aminododecanoyl))-2-oleoyl-*sn*-glycero-3-phosphoethanolamine was included in the t-SNARE liposomes, and WT VAMP2 was replaced with a VAMP2NTD-TolA chimera in the v-SNARE liposomes. Because membrane docking is mediated by the N-terminal domains (NTDs) of SNAREs, the VAMP2NTD-TolA chimera was ideally suited for monitoring the upstream docking step. The biotin-labeled t-SNARE liposomes were incubated with avidin-conjugated Sepharose beads at room temperature for 1 h. The bead-bound t-SNARE liposomes were then used to pull down rhodamine-labeled v-SNARE liposomes. The pulldown reactions were performed at 4 °C in the presence or absence of 5 μM Munc18-1. After washing three times with the reconstitution buffer, CHAPS was added to a final concentration of 1% to solubilize the bead-bound liposomes. After removing avidin beads by centrifugation, rhodamine fluorescence in the supernatant was measured in a BioTek microplate reader. The binding reaction containing biotin-labeled, protein-free liposomes was used as a negative control to obtain the background fluorescence signal. The background rhodamine fluorescence was subtracted from other binding reactions to calculate SNARE-mediated liposome docking.

Generation of iN cells

Human iPSCs (clone I_{50}-2) were generated from human adult fibroblasts (ATCC) using a RNA-based reprogramming method and were characterized previously (64). The iPSCs were programmed into iN cells following a procedure described previously (53). The iPSCs were cultured on Matrigel (BD Biosciences)-coated coverslips in Essential 8 medium (Life Technologies, Inc.) supplemented with 10 μM Y-27632 dihydrochloride (Tocris). Lentivirus particles containing the Ngn2 expression gene were added to Essential 8 medium containing 8 μg/ml Polybrene. After 24 h (day 0), the culture media were replaced with N2/DMEM/F12/NEAA (Life Technologies) containing human brain-derived neurotrophic factor (10 μg/liter; PeproTech), human NT-3 (10 μg/liter; PeproTech), and mouse laminin (0.2 mg/liter; Life Technologies). Meanwhile, doxycycline (2 μg/ml; Clontech) was added to induce TetO gene expression. On day 1, 1 μg/ml puromycin was added to select for transduced cells. After 24 h (day 2), the cells were fed with Neurobasal medium (Gibco), and mouse glia cells were added. The iN cells were analyzed between day 16 and day 21.

CRISPR/Cas9 genome editing

The lentiCRISPR plasmid (Addgene) was used to delete the *MUNC18-1* gene in iPSCs. For gene KO using one gRNA, the following guide sequence targeting the second exon of the *MUNC18-1* gene was selected: 5′-GATAAAGAAGGTCAAGAAGAAGG-3′.

For gene knockout using double gRNAs, the following guide sequences were used: 5′-ATCCACCACCAGCACCTGCAAGG-3′ and 5′-CTGTTGTCGGAGAGAGTAAGTGG-3′.

The guide sequences were individually subcloned into the BsmBI sites of the plentiCRISPR vector. Lentiviral particles prepared with the lentiCRISPR plasmids were used to infect iPSCs. On the next day, the cells were treated with 1 μg/ml puromycin for 24 h to select for transduced cells. CRISPR/Cas9 is expected to induce compound heterozygous mutations that are functionally equivalent to homozygous KO (65). In gene rescue experiments, the rat *Munc18-1* gene was subcloned into the BamHI and KpnI sites of the TRC2 pLKO vector. To prevent cleavage of the rescue gene by Cas9 in the single gRNA CRISPR KO, silent mutations were introduced into the rat *Munc18-1* rescue gene near the PAM site using the following mutagenesis primer: 5′-GCATGATGTTATCAAGAAGGTGAAAAAAAAAGGCGAGTGGAAGGTGCTGGTG-3′. In CRISPR KO using two gRNAs, the rescue gene was not mutated, because neither of the gRNAs targets the *Munc18-1 rescue* gene.

Immunoblotting and immunostaining

For immunoblotting, total cellular proteins were extracted by SDS sample buffer and resolved on SDS-PAGE. After being transferred onto polyvinylidene difluoride membranes, VAMP2 and syntaxin-1 were probed as described for the trans-SNARE assembly assays. Munc18-1 expression was measured by using monoclonal anti-Munc18-1 antibodies (clone 31/Munc-18, BD Biosciences). Expression of α-tubulin was measured using monoclonal anti-α-tubulin antibodies (clone TU-01, BioLegend).

For immunostaining, cells were fixed by 4% paraformaldehyde and permeabilized using 0.2% Triton X-100. After blocking with 10% BSA, MAP2 was stained using mouse monoclonal anti-MAP2 antibodies (Sigma, M9942) and goat rhodamine-conjugated secondary antibodies (Jackson ImmunoResearch, 115-025-062). Images were acquired on a Carl Zeiss 3i Marianas spinning disk confocal microscope and processed using ImageJ.

Electrophysiological recordings

EPSCs and mEPSCs were recorded in iN cells using our established procedures (52). Evoked synaptic transmission was triggered by 1-ms current injections using a concentric bipolar microelectrode (FHC; model CBAEC75) placed about 100–150 μm from the cell bodies of patched iN cells. The extracellular

stimuli were manipulated using an isolated pulse stimulator (World Precision Instruments). The evoked responses were measured by whole-cell recordings using a Multiclamp 700B amplifier (Molecular Devices). The whole-cell pipette solution contained 135 mM CsCl, 10 mM HEPES-CsOH (pH 7.25), 0.5 mM EGTA, 2 mM $MgCl_2$, 0.4 mM NaCl-GTP, and 4 mM NaCl-ATP. The bath solution contained 140 mM NaCl, 5 mM KCl, 2 mM $CaCl_2$, 0.8 $MgCl_2$, 10 mM HEPES-NaOH (pH 7.4), and 10 mM glucose. The mEPSCs of the neurons were sampled at 10 kHz in the presence of 1 μM tetrodotoxin (Sigma). The resistance of pipettes was 3–5 megaohms. The series resistance was adjusted to 8–10 megaohms once the whole-cell configuration was achieved.

The detailed numbers of cultures and neurons are listed in Table S1. The electrophysiological data were processed using the pClamp 10 software (Molecular Devices). For statistical calculations, all data are shown as mean ± S.E. The *p* values were calculated using Student's *t* test. In gene rescue experiments, all data are compared with the results of WT cells.

Author contributions—C. S. data curation; C. S. and Y. L. formal analysis; C. S., Y. L., H. Y., and D. R. G. investigation; C. S., H. Y., and D. R. G. methodology; I. K., G. B., C. Z., M. H. S., and J. S. resources; M. H. S. validation; M. H. S. writing-original draft; J. S. conceptualization; J. S. supervision; J. S. funding acquisition; J. S. writing-review and editing.

Acknowledgments—We thank Dr. Keming Zhou for helpful discussions, Dr. Thomas Südhof for providing the iN programming plasmids, and Dr. Jolien Tyler for assistance with confocal imaging.

References

1. Südhof, T. C., and Rothman, J. E. (2009) Membrane fusion: grappling with SNARE and SM proteins. *Science* **323,** 474–477 CrossRef Medline
2. Wickner, W. (2010) Membrane fusion: five lipids, four SNAREs, three chaperones, two nucleotides, and a Rab, all dancing in a ring on yeast vacuoles. *Annu. Rev. Cell Dev. Biol.* **26,** 115–136 CrossRef Medline
3. Baker, R. W., and Hughson, F. M. (2016) Chaperoning SNARE assembly and disassembly. *Nat. Rev. Mol. Cell Biol.* **17,** 465–479 CrossRef Medline
4. Söllner, T., Whiteheart, S. W., Brunner, M., Erdjument-Bromage, H., Geromanos, S., Tempst, P., and Rothman, J. E. (1993) SNAP receptors implicated in vesicle targeting and fusion. *Nature* **362,** 318–324 CrossRef Medline
5. Weber, T., Zemelman, B. V., McNew, J. A., Westermann, B., Gmachl, M., Parlati, F., Söllner, T. H., and Rothman, J. E. (1998) SNAREpins: minimal machinery for membrane fusion. *Cell* **92,** 759–772 CrossRef Medline
6. Jahn, R., and Scheller, R. H. (2006) SNAREs–engines for membrane fusion. *Nature Rev. Mol. Cell Biol.* **7,** 631–643 CrossRef Medline
7. Ungar, D., and Hughson, F. M. (2003) SNARE protein structure and function. *Annu. Rev. Cell Dev. Biol.* **19,** 493–517 CrossRef Medline
8. Zhou, P., Bacaj, T., Yang, X., Pang, Z. P., and Südhof, T. C. (2013) Lipid-anchored SNAREs lacking transmembrane regions fully support membrane fusion during neurotransmitter release. *Neuron* **80,** 470–483 CrossRef Medline
9. Xu, H., Zick, M., Wickner, W. T., and Jun, Y. (2011) A lipid-anchored SNARE supports membrane fusion. *Proc. Natl. Acad. Sci. U.S.A.* **108,** 17325–17330 CrossRef Medline
10. Gao, Y., Zorman, S., Gundersen, G., Xi, Z., Ma, L., Sirinakis, G., Rothman, J. E., and Zhang, Y. (2012) Single reconstituted neuronal SNARE complexes zipper in three distinct stages. *Science* **337,** 1340–1343 CrossRef Medline
11. Reese, C., Heise, F., and Mayer, A. (2005) Trans-SNARE pairing can precede a hemifusion intermediate in intracellular membrane fusion. *Nature* **436,** 410–414 CrossRef Medline
12. Ellena, J. F., Liang, B., Wiktor, M., Stein, A., Cafiso, D. S., Jahn, R., and Tamm, L. K. (2009) Dynamic structure of lipid-bound synaptobrevin suggests a nucleation-propagation mechanism for trans-SNARE complex formation. *Proc. Natl. Acad. Sci. U.S.A.* **106,** 20306–20311 CrossRef Medline
13. Hata, Y., Slaughter, C. A., and Südhof, T. C. (1993) Synaptic vesicle fusion complex contains unc-18 homologue bound to syntaxin. *Nature* **366,** 347–351 CrossRef Medline
14. Dulubova, I., Khvotchev, M., Liu, S., Huryeva, I., Südhof, T. C., and Rizo, J. (2007) Munc18-1 binds directly to the neuronal SNARE complex. *Proc. Natl. Acad. Sci. U.S.A.* **104,** 2697–2702 CrossRef Medline
15. Novick, P., and Schekman, R. (1979) Secretion and cell-surface growth are blocked in a temperature-sensitive mutant of Saccharomyces cerevisiae. *Proc. Natl. Acad. Sci. U.S.A.* **76,** 1858–1862 CrossRef Medline
16. Pevsner, J., Hsu, S. C., and Scheller, R. H. (1994) n-Sec1: a neural-specific syntaxin-binding protein. *Proc. Natl. Acad. Sci. U.S.A.* **91,** 1445–1449 CrossRef Medline
17. Garcia, E. P., Gatti, E., Butler, M., Burton, J., and De Camilli, P. (1994) A rat brain Sec1 homologue related to Rop and UNC18 interacts with syntaxin. *Proc. Natl. Acad. Sci. U.S.A.* **91,** 2003–2007 CrossRef Medline
18. Shen, J., Tareste, D. C., Paumet, F., Rothman, J. E., and Melia, T. J. (2007) Selective activation of cognate SNAREpins by Sec1/Munc18 proteins. *Cell* **128,** 183–195 CrossRef Medline
19. Rizo, J., and Südhof, T. C. (2012) The membrane fusion enigma: SNAREs, Sec1/Munc18 proteins, and their accomplices—guilty as charged? *Annu. Rev. Cell Dev. Biol.* **28,** 279–308 CrossRef Medline
20. Sudhof, T. C. (2004) The synaptic vesicle cycle. *Annu. Rev. Neurosci.* **27,** 509–547 CrossRef Medline
21. Jackson, M. B., and Chapman, E. R. (2006) Fusion pores and fusion machines in Ca^{2+}-triggered exocytosis. *Annu. Rev. Biophys. Biomol. Struct.* **35,** 135–160 CrossRef Medline
22. Bennett, M. K., Calakos, N., and Scheller, R. H. (1992) Syntaxin: a synaptic protein implicated in docking of synaptic vesicles at presynaptic active zones. *Science* **257,** 255–259 CrossRef Medline
23. Elferink, L. A., Trimble, W. S., and Scheller, R. H. (1989) Two vesicle-associated membrane protein genes are differentially expressed in the rat central nervous system. *J. Biol. Chem.* **264,** 11061–11064 Medline
24. Oyler, G. A., Higgins, G. A., Hart, R. A., Battenberg, E., Billingsley, M., Bloom, F. E., and Wilson, M. C. (1989) The identification of a novel synaptosomal-associated protein, SNAP-25, differentially expressed by neuronal subpopulations. *J. Cell Biol.* **109,** 3039–3052 CrossRef Medline
25. Südhof, T. C., Baumert, M., Perin, M. S., and Jahn, R. (1989) A synaptic vesicle membrane protein is conserved from mammals to *Drosophila*. *Neuron* **2,** 1475–1481 CrossRef Medline
26. Sutton, R. B., Fasshauer, D., Jahn, R., and Brunger, A. T. (1998) Crystal structure of a SNARE complex involved in synaptic exocytosis at 2.4 Å resolution. *Nature* **395,** 347–353 CrossRef Medline
27. Weimer, R. M., Richmond, J. E., Davis, W. S., Hadwiger, G., Nonet, M. L., and Jorgensen, E. M. (2003) Defects in synaptic vesicle docking in unc-18 mutants. *Nat. Neurosci.* **6,** 1023–1030 CrossRef Medline
28. Verhage, M., Maia, A. S., Plomp, J. J., Brussaard, A. B., Heeroma, J. H., Vermeer, H., Toonen, R. F., Hammer, R. E., van den Berg, T. K., Missler, M., Geuze, H. J., and Südhof, T. C. (2000) Synaptic assembly of the brain in the absence of neurotransmitter secretion. *Science* **287,** 864–869 CrossRef Medline
29. Ma, L., Rebane, A. A., Yang, G., Xi, Z., Kang, Y., Gao, Y., and Zhang, Y. (2015) Munc18-1-regulated stage-wise SNARE assembly underlying synaptic exocytosis. *eLife* **4,** e09580 CrossRef Medline
30. Rizo, J., and Xu, J. (2015) The synaptic vesicle release machinery. *Annu. Rev. Biophys.* **44,** 339–367 CrossRef Medline
31. Ma, C., Su, L., Seven, A. B., Xu, Y., and Rizo, J. (2013) Reconstitution of the vital functions of Munc18 and Munc13 in neurotransmitter release. *Science* **339,** 421–425 CrossRef Medline

32. Rodkey, T. L., Liu, S., Barry, M., and McNew, J. A. (2008) Munc18a scaffolds SNARE assembly to promote membrane fusion. *Mol. Biol. Cell* **19,** 5422–5434 CrossRef Medline
33. Munch, A. S., Kedar, G. H., van Weering, J. R., Vazquez-Sanchez, S., He, E., André, T., Braun, T., Söllner, T. H., Verhage, M., and Sørensen, J. B. (2016) Extension of helix 12 in Munc18-1 induces vesicle priming. *J. Neurosci.* **36,** 6881–6891 CrossRef Medline
34. Lobingier, B. T., Nickerson, D. P., Lo, S. Y., and Merz, A. J. (2014) SM proteins Sly1 and Vps33 co-assemble with Sec17 and SNARE complexes to oppose SNARE disassembly by Sec18. *Elife* **3,** e02272 CrossRef Medline
35. Yu, H., Rathore, S. S., Lopez, J. A., Davis, E. M., James, D. E., Martin, J. L., and Shen, J. (2013) Comparative studies of Munc18c and Munc18-1 reveal conserved and divergent mechanisms of Sec1/Munc18 proteins. *Proc. Natl. Acad. Sci. U.S.A.* **110,** E3271–E3280 CrossRef Medline
36. Shen, J., Rathore, S. S., Khandan, L., and Rothman, J. E. (2010) SNARE bundle and syntaxin N-peptide constitute a minimal complement for Munc18-1 activation of membrane fusion. *J. Cell Biol.* **190,** 55–63 CrossRef Medline
37. Rathore, S. S., Bend, E. G., Yu, H., Hammarlund, M., Jorgensen, E. M., and Shen, J. (2010) Syntaxin N-terminal peptide motif is an initiation factor for the assembly of the SNARE-Sec1/Munc18 membrane fusion complex. *Proc. Natl. Acad. Sci. U.S.A.* **107,** 22399–22406 CrossRef Medline
38. Baker, R. W., Jeffrey, P. D., Zick, M., Phillips, B. P., Wickner, W. T., and Hughson, F. M. (2015) A direct role for the Sec1/Munc18-family protein Vps33 as a template for SNARE assembly. *Science* **349,** 1111–1114 CrossRef Medline
39. Parisotto, D., Malsam, J., Scheutzow, A., Krause, J. M., and Söllner, T. H. (2012) SNAREpin assembly by Munc18-1 requires previous vesicle docking by synaptotagmin 1. *J. Biol. Chem.* **287,** 31041–31049 CrossRef Medline
40. Shin, Y. K. (2013) Two gigs of Munc18 in membrane fusion. *Proc. Natl. Acad. Sci. U.S.A.* **110,** 14116–14117 CrossRef Medline
41. Furgason, M. L., MacDonald, C., Shanks, S. G., Ryder, S. P., Bryant, N. J., and Munson, M. (2009) The N-terminal peptide of the syntaxin Tlg2p modulates binding of its closed conformation to Vps45p. *Proc. Natl. Acad. Sci. U.S.A.* **106,** 14303–14308 CrossRef Medline
42. Burkhardt, P., Hattendorf, D. A., Weis, W. I., and Fasshauer, D. (2008) Munc18a controls SNARE assembly through its interaction with the syntaxin N-peptide. *EMBO J.* **27,** 923–933 CrossRef Medline
43. Bracher, A., and Weissenhorn, W. (2002) Structural basis for the Golgi membrane recruitment of Sly1p by Sed5p. *EMBO J.* **21,** 6114–6124 CrossRef Medline
44. Hu, S. H., Latham, C. F., Gee, C. L., James, D. E., and Martin, J. L. (2007) Structure of the Munc18c/Syntaxin4 N-peptide complex defines universal features of the N-peptide binding mode of Sec1/Munc18 proteins. *Proc. Natl. Acad. Sci. U.S.A.* **104,** 8773–8778 CrossRef Medline
45. Yamaguchi, T., Dulubova, I., Min, S. W., Chen, X., Rizo, J., and Südhof, T. C. (2002) Sly1 binds to Golgi and ER syntaxins via a conserved N-terminal peptide motif. *Dev. Cell* **2,** 295–305 CrossRef Medline
46. Zhou, P., Pang, Z. P., Yang, X., Zhang, Y., Rosenmund, C., Bacaj, T., and Sudhof, T. C. (2013) Syntaxin-1 N-peptide and H(abc)-domain perform distinct essential functions in synaptic vesicle fusion. *EMBO J.* **32,** 159–171 CrossRef Medline
47. Johnson, J. R., Ferdek, P., Lian, L. Y., Barclay, J. W., Burgoyne, R. D., and Morgan, A. (2009) Binding of UNC-18 to the N-terminus of syntaxin is essential for neurotransmission in *Caenorhabditis elegans*. *Biochem. J.* **418,** 73–80 CrossRef Medline
48. McEwen, J. M., and Kaplan, J. M. (2008) UNC-18 promotes both the anterograde trafficking and synaptic function of syntaxin. *Mol. Biol. Cell* **19,** 3836–3846 CrossRef Medline
49. Meijer, M., Burkhardt, P., de Wit, H., Toonen, R. F., Fasshauer, D., and Verhage, M. (2012) Munc18-1 mutations that strongly impair SNARE-complex binding support normal synaptic transmission. *EMBO J.* **31,** 2156–2168 CrossRef Medline
50. Park, S., Bin, N. R., Michael Rajah, M., Kim, B., Chou, T. C., Kang, S. Y., Sugita, K., Parsaud, L., Smith, M., Monnier, P. P., Ikura, M., Zhen, M., and Sugita, S. (2016) Conformational states of syntaxin-1 govern the necessity of N-peptide binding in exocytosis of PC12 cells and *Caenorhabditis elegans*. *Mol. Biol. Cell* **27,** 669–685 CrossRef Medline
51. Malintan, N. T., Nguyen, T. H., Han, L., Latham, C. F., Osborne, S. L., Wen, P. J., Lim, S. J., Sugita, S., Collins, B. M., and Meunier, F. A. (2009) Abrogating Munc18-1-SNARE complex interaction has limited impact on exocytosis in PC12 cells. *J. Biol. Chem.* **284,** 21637–21646 CrossRef Medline
52. Shen, C., Rathore, S. S., Yu, H., Gulbranson, D. R., Hua, R., Zhang, C., Schoppa, N. E., and Shen, J. (2015) The trans-SNARE-regulating function of Munc18-1 is essential to synaptic exocytosis. *Nat. Commun.* **6,** 8852 CrossRef Medline
53. Zhang, Y., Pak, C., Han, Y., Ahlenius, H., Zhang, Z., Chanda, S., Marro, S., Patzke, C., Acuna, C., Covy, J., Xu, W., Yang, N., Danko, T., Chen, L., Wernig, M., and Südhof, T. C. (2013) Rapid single-step induction of functional neurons from human pluripotent stem cells. *Neuron* **78,** 785–798 CrossRef Medline
54. Kondo, T., Asai, M., Tsukita, K., Kutoku, Y., Ohsawa, Y., Sunada, Y., Imamura, K., Egawa, N., Yahata, N., Okita, K., Takahashi, K., Asaka, I., Aoi, T., Watanabe, A., Watanabe, K., *et al.* (2013) Modeling Alzheimer's disease with iPSCs reveals stress phenotypes associated with intracellular Aβ and differential drug responsiveness. *Cell Stem Cell* **12,** 487–496 CrossRef Medline
55. Patzke, C., Han, Y., Covy, J., Yi, F., Maxeiner, S., Wernig, M., and Südhof, T. C. (2015) Analysis of conditional heterozygous STXBP1 mutations in human neurons. *J. Clin. Invest.* **125,** 3560–3571 CrossRef Medline
56. Lai, Y., Choi, U. B., Leitz, J., Rhee, H. J., Lee, C., Altas, B., Zhao, M., Pfuetzner, R. A., Wang, A. L., Brose, N., Rhee, J., and Brunger, A. T. (2017) Molecular mechanisms of synaptic vesicle priming by Munc13 and Munc18. *Neuron* **95,** 591–607.e10 CrossRef Medline
57. Gulbranson, D. R., Davis, E. M., Demmitt, B. A., Ouyang, Y., Ye, Y., Yu, H., and Shen, J. (2017) RABIF/MSS4 is a Rab-stabilizing holdase chaperone required for GLUT4 exocytosis. *Proc. Natl. Acad. Sci. U.S.A.* **114,** E8224–E8233 CrossRef Medline
58. Jewell, J. L., Oh, E., Ramalingam, L., Kalwat, M. A., Tagliabracci, V. S., Tackett, L., Elmendorf, J. S., and Thurmond, D. C. (2011) Munc18c phosphorylation by the insulin receptor links cell signaling directly to SNARE exocytosis. *J. Cell Biol.* **193,** 185–199 CrossRef Medline
59. Bryant, N. J., Govers, R., and James, D. E. (2002) Regulated transport of the glucose transporter GLUT4. *Nature reviews. Mol. Cell Biol.* **3,** 267–277 CrossRef Medline
60. Lee, Y. K., and Cowan, C. A. (2014) Differentiation of white and brown adipocytes from human pluripotent stem cells. *Methods Enzymol.* **538,** 35–47 CrossRef Medline
61. Ahfeldt, T., Schinzel, R. T., Lee, Y. K., Hendrickson, D., Kaplan, A., Lum, D. H., Camahort, R., Xia, F., Shay, J., Rhee, E. P., Clish, C. B., Deo, R. C., Shen, T., Lau, F. H., Cowley, A., *et al.* (2012) Programming human pluripotent stem cells into white and brown adipocytes. *Nat. Cell Biol.* **14,** 209–219 CrossRef Medline
62. Rao, L., Qian, Y., Khodabukus, A., Ribar, T., and Bursac, N. (2018) Engineering human pluripotent stem cells into a functional skeletal muscle tissue. *Nat. Commun.* **9,** 126 CrossRef Medline
63. Yu, H., Rathore, S. S., Shen, C., Liu, Y., Ouyang, Y., Stowell, M. H., and Shen, J. (2015) Reconstituting intracellular vesicle fusion reactions: the essential role of macromolecular crowding. *J. Am. Chem. Soc.* **137,** 12873–12883 CrossRef Medline
64. Yu, H., Liu, Y., Gulbranson, D. R., Paine, A., Rathore, S. S., and Shen, J. (2016) Extended synaptotagmins are Ca^{2+}-dependent lipid transfer proteins at membrane contact sites. *Proc. Natl. Acad. Sci. U.S.A.* **113,** 4362–4367 CrossRef Medline
65. Shalem, O., Sanjana, N. E., and Zhang, F. (2015) High-throughput functional genomics using CRISPR-Cas9. *Nat. Rev. Genet.* **16,** 299–311 CrossRef Medline
66. Yu, H., Shen, C., Liu, Y., Menasche, B. L., Ouyang, Y., Stowell, M. H. B., and Shen, J. (2018) SNARE zippering requires activation by SNARE-like peptides in Sec1/Munc18 proteins. *Proc. Natl. Acad. Sci. U.S.A.* **115,** E8421–E8429 CrossRef Medline